

Chiral flux phase in the Kagome superconductor AV_3Sb_5

Xilin Feng,^{1,2} Kun Jiang,^{1,*} Ziqiang Wang,³ and Jiangping Hu^{1,4,†}

¹Beijing National Laboratory for Condensed Matter Physics and Institute of Physics, Chinese Academy of Sciences, Beijing 100190, China

²School of Physical Sciences, University of Chinese Academy of Sciences, Beijing 100190, China

³Department of Physics, Boston College, Chestnut Hill, MA 02467, USA

⁴Kavli Institute of Theoretical Sciences, University of Chinese Academy of Sciences, Beijing 100190, China

(Dated: May 7, 2021)

We argue that the topological charge density wave phase in the quasi-2D Kagome superconductor AV_3Sb_5 is a chiral flux phase. Considering the symmetry of the Kagome lattice, we show that the chiral flux phase has the lowest energy among those states which exhibit 2×2 charge orders observed experimentally. This state breaks the time-reversal symmetry and displays anomalous Hall effect. The explicit pattern of the density of this state in real space is calculated. These results are supported by recent experiments and suggest that these materials are a new platform to investigate the interplay between topology, superconductivity and electron-electron correlations.

I. INTRODUCTION

Owing to its special geometry, materials with a Kagome lattice structure have become very attractive systems to investigate many-body correlation physics. For example, the geometry frustration in Kagome magnetism is one of the promising routes towards the quantum spin liquid [1–3]. The electronic structure of the Kagome lattice also hosts Dirac cones and flat bands, which gives rise to many intriguing quantum phenomena including nontrivial flat-band responses, tunable Dirac cone etc. [4–9]. Additionally, those Kagome materials also exhibit rich topological physics including anomalous and quantum anomalous Hall, Z_2 topological insulator, etc [10–12]. All these fantastic quantum properties make the Kagome lattice being an important platform to explore novel physics.

Recently, the newly discovered quasi-2 dimensional (2D) superconductors AV_3Sb_5 ($A=K,Rb,Cs$) may become a very unique system to study the Kagome physics [13–19]. Up to date, the superconductivity of AV_3Sb_5 shows nodal features [17, 20, 21]. The study of Josephson junction also provides evidence for possible spin-triplet supercurrent [22]. Besides the superconducting ground state, a topological 2×2 charge density wave state (CDW) was also observed in KV_3Sb_5 by scanning tunneling microscopy (STM) under magnetic field [23], which may hold the key to explain the observed anomalous Hall effect [24, 25] and topological edge state [22].

These experimental results suggest that AV_3Sb_5 are intriguing Kagome materials. However, these experimental findings still lack theoretical understanding. In this work, we will focus on the CDW order observed in the normal state. We show that a chiral flux phase (CFP), which provides a 2×2 topological CDW order, is a natural candidate to explain observed experimental results. The phase is the lowest energy state that satisfies the symmetry constraints of the Kagome lattice. The CFP phase breaks the time reversal symmetry \mathcal{T} and gives rise to the quantum anomalous Hall response.

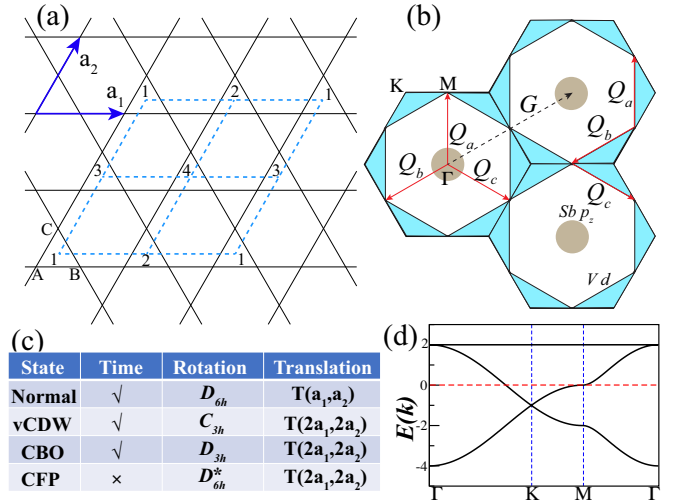


FIG. 1: (a) The Kagome lattice and its translation vector \mathbf{a}_1 and \mathbf{a}_2 . In each unit cell, the sublattice is labeled as A,B,C. The dashed blue lattice is the triangular lattice formed by the unit cell. And the 2×2 unit cell is also plotted. The sub-unit cell for the 2×2 CDW order is also labeled as 1, 2, 3, 4. (b) The BZ for Kagome lattice. There is one $Sb p_z$ FS (grey circle) around the Γ point and the $v d$ FS (blue triangles) around the M point. The M point FS is around the $1/4$ zone filling. The inter-scattering vectors between M points are indicated by Q_a, Q_b, Q_c . (c) Table for symmetry properties for the normal state and three 2×2 symmetry breaking states, including time reversal symmetry \mathcal{T} , point group and translation group. The effective point group D_{6h}^* is equal to $\{C_{6h}, C_2', \mathcal{T}C_{6h}\}$. (d) The band structure for the nearest neighbor Kagome lattice at $5/4$ filling.

II. TIGHT-BINDING MODEL

As illustrated in Fig. 1a, each unit cell of Kagome lattice contains three sublattices, labeled as A, B, C. And the unit cell forms a triangular lattice with translation vector $\mathbf{a}_1 = (1, 0)$ and $\mathbf{a}_2 = (\frac{1}{2}, \frac{\sqrt{3}}{2})$. This translation group is labeled as $T(\mathbf{a}_1, \mathbf{a}_2)$. And the point group for the Kagome lattice is D_{6h} , as summarized in Fig. 1c. The 2×2 CDW order quadruply enlarges the unit cell, as indicated by the blue dash lattice in Fig. 1a. Each unit cell inside the quadruple order is also labeled as 1, 2, 3, 4. The density functional

*Electronic address: jiangkun@iphy.ac.cn

†Electronic address: jphu@iphy.ac.cn

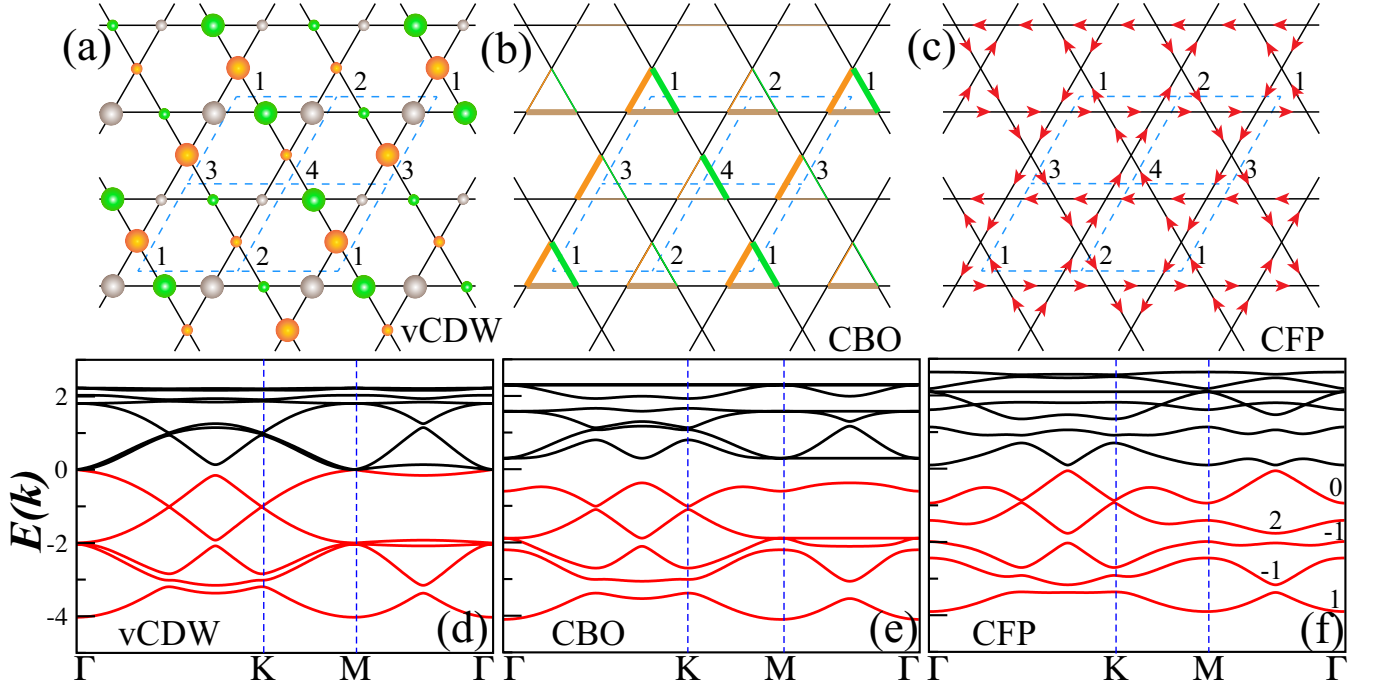


FIG. 2: Three charge orders and their corresponding band structures. (a) the charge configuration for chiral charge density wave (cCDW). (b) the real bond order configuration for charge bond order (CBO). (c) the hopping flux configuration for chiral flux phase (CFP). (d) the band structures for cCDW with $\lambda = 0.3$. (e) the band structures for CBO with $\lambda = 0.3$. (f) the band structures for CFP with $\lambda = 0.3$. All the occupied bands are highlight by red for (d), (e), (f). The Chern number for the occupied bands of CFP is also shown in (f).

theory (DFT) calculation shows the normal state of Kagome AV_3Sb_5 is a quasi-2D metal, which is excellently captured by the angle-resolved photoemission spectroscopy (ARPES) measurements [14]. Therefore, the AV_3Sb_5 lies in a weak correlation regime and can be effectively described by a 2D model. Based on DFT and ARPES results, we find that the in-plane Sb p_z orbital forms one electron pocket around the Γ point and the V d orbitals form multiple FSs around the M points, as illustrated in Fig. 1b. Importantly, the V d band FSs touch the van Hove (vH) M points. The inter-scatterings between three vH points give us three important wave vectors $\mathbf{Q}_a = \{0, \frac{2\pi}{\sqrt{3}}\}$, $\mathbf{Q}_b = \{-\pi, -\frac{\pi}{\sqrt{3}}\}$ and $\mathbf{Q}_c = \{\pi, -\frac{\pi}{\sqrt{3}}\}$, which is widely believed to be the reason for CDW in AV_3Sb_5 . Hence, this 2×2 order is also called the 3Q quadruple order. The STM quasiparticle interference (QPI) results also show the 3Q scattering between M points in addition to the Γ point intra-FS scattering [20, 21]. Therefore, to capture the main physics of the topological CDW in AV_3Sb_5 , we can use a minimum single orbital model to study the electronic physics.

The nearest neighbor tight-binding model for Kagome lattice in the basis of $c_k = (c_{k,A}, c_{k,B}, c_{k,C})$ can be written as $H_0 = \sum_k c_k^\dagger H_k c_k$, where

$$H_k = \begin{bmatrix} -\mu & -2t \cos(k_1/2) & -2t \cos(k_2/2) \\ -2t \cos(k_1/2) & -\mu & -2t \cos(k_3/2) \\ -2t \cos(k_2/2) & -2t \cos(k_3/2) & -\mu \end{bmatrix} \quad (1)$$

and $k_1 = k_x$, $k_2 = \frac{1}{2}k_x + \frac{\sqrt{3}}{2}k_y$, and $k_3 = -\frac{1}{2}k_x + \frac{\sqrt{3}}{2}k_y$. μ is the chemical potential and the hopping t is chosen to be 1 as the energy unit. The band structure for Kagome model is

shown in Fig. 1d and the electron filling is tuned to the $5/4$ VH filling. The corresponding FS agrees with the FS plotted in Fig. 1b.

III. 3Q INSTABILITY AND CHIRAL FLUX PHASE

As described above, the 2×2 CDW in AV_3Sb_5 is widely believed to stem from the multiple Q scatterings between the Kagome VH points, which breaks the translation group down to $T(2\mathbf{a}_1, 2\mathbf{a}_2)$. Actually, these multiple Q FS instability at $3/4$ or $1/4$ zone filling for hexagonal lattices stems from the seminar discussion in triangular lattice [26], where the 3Q non-coplanar chiral spin density wave (SDW) order is found to be the leading instability in the Kondo lattice model and the Hubbard model. The chiral SDW order parameter $\mathbf{S}(\mathbf{r})$ can be written as

$$\mathbf{S}(\mathbf{r}) = S(\cos(\mathbf{Q}_a \cdot \mathbf{r}), \cos(\mathbf{Q}_b \cdot \mathbf{r}), \cos(\mathbf{Q}_c \cdot \mathbf{r})) \quad (2)$$

where the spin vector is defined as (s_x, s_y, s_z) in the three directions. The four spin vectors of this quadrupled SDW order form a tetrahedron AFM at the triangular lattice. Because of the non-zero spin chirality $\mathbf{S}_1 \cdot (\mathbf{S}_2 \times \mathbf{S}_3)$, this quadruple order breaks the time-reversal symmetry and causes a quantum anomalous Hall effect [26]. Besides this chiral SDW order, various FS instabilities, such as $d + id$ superconductivity, have been widely studied in the honeycomb and Kagome lattices by mean-field theory [27–30], renormalization group (RG) [31], functional RG [32–35], and density matrix RG [36], etc.

For AV_3Sb_5 , the neutron scattering and the muon spin spectroscopy find little evidence for local magnetic moments or long-range magnetic orders [13, 37]. Therefore, we will only consider the spontaneous symmetric breaking in the charge channel. In order to construct a 2×2 order, the order parameter must utilize all the three Q scattering vectors, which implies the order parameter must contain three components in analogy to the spin (s_x, s_y, s_z) . The key idea for 2×2 charge order is finding this three-component vector. Fortunately, the Kagome lattice still has the sublattice degree of freedom beside the spin space. We can use the three sublattices A, B, C to form a three-component vector.

Obviously, the first choice is the charge density for each sublattice

$$\hat{\mathbf{n}}(\mathbf{R}) = (\hat{n}_A, \hat{n}_B, \hat{n}_C) \quad (3)$$

where the \mathbf{R} is the coordinate for the unit cell formed by the sublattices A, B, C. We name this charge order as the vector charge density wave (vCDW). The order parameter for this vector can be written as

$$\Delta_{vCDW}(\mathbf{R}) = \lambda(\cos(\mathbf{Q}_a \cdot \mathbf{R}), \cos(\mathbf{Q}_b \cdot \mathbf{R}), \cos(\mathbf{Q}_c \cdot \mathbf{R})) \quad (4)$$

where the λ is the coupling strength. Then, the charge order Hamiltonian can be written as

$$H = H_0 - \sum_{\mathbf{R}} \Delta_{vCDW} \cdot \hat{\mathbf{n}}(\mathbf{R}) \quad (5)$$

The charge density for this vCDW order is illustrated in Fig. 2a. The corresponding band structures are also plotted in Fig. 2d. From the band structures in Fig. 2d, we find the vCDW order can not lift the M point degeneracy from the 3Q folding at $\lambda = 0.3$. Hence, this state can not be the ground state.

Besides the charge density $\hat{\mathbf{n}}(\mathbf{R})$, the hopping bonds inside each unit cell can also form a vector

$$\hat{\mathbf{O}}(\mathbf{R}) = (c_A^\dagger c_B, c_B^\dagger c_C, c_C^\dagger c_A) \quad (6)$$

More specifically, there are two choices for the hopping bond order parameters, real or imaginary. If the order parameter is real, a charge bond order (CBO) is formed, as illustrated in Fig. 2b. The order parameter for this order can be written as

$$\Delta_{CBO}(\mathbf{R}) = \lambda(\cos(\mathbf{Q}_a \cdot \mathbf{R}), \cos(\mathbf{Q}_b \cdot \mathbf{R}), \cos(\mathbf{Q}_c \cdot \mathbf{R})) \quad (7)$$

Then, the charge order Hamiltonian can be written as

$$H = H_0 - \sum_{\mathbf{R}} \Delta_{CBO} \cdot \hat{\mathbf{O}}(\mathbf{R}) \quad (8)$$

The band structure for CBO at $\lambda = 0.3$ is shown in Fig. 2b. The CBO opens a large gap at the M point becoming a possible charge order solution. And this CBO is similar to the CBO proposed in Ref. [35].

On the other hand, if the order parameter is imaginary, a chiral flux phase is formed, which can be written as

$$\Delta_{CFP}(\mathbf{R}) = i\lambda(\cos(\mathbf{Q}_a \cdot \mathbf{R}), \cos(\mathbf{Q}_b \cdot \mathbf{R}), \cos(\mathbf{Q}_c \cdot \mathbf{R})) \quad (9)$$

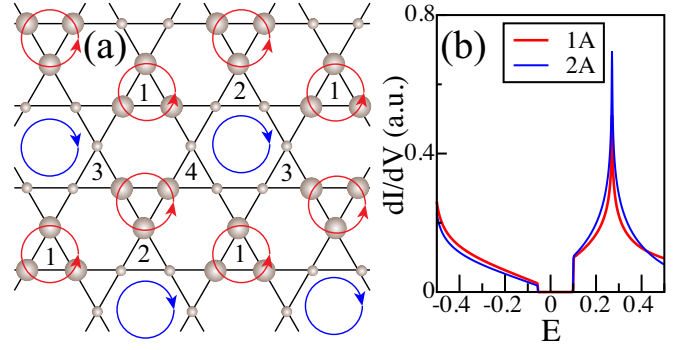


FIG. 3: (a) The relative charge configuration for CFP. The charge density for the anti-clockwise flux triangular sites is larger than the charge density for the clockwise flux hexagonal sites. (b) The tunneling density of states for site 1A and site 2A.

As the current must conserve at each lattice site without charge accumulation, we can determine the chiral flux phase, as shown in Fig. 2c. Adding this order parameter and the remaining terms due to current constraint, the band structure for CFP Hamiltonian is obtained in Fig. 2f. The CFP also opens gap on the FSs at the M point and lifts most of the degeneracy below the Fermi level. More importantly, the ground state energy for CFP is 0.195t lower than the CBO per unit cell and 0.435t lower than the CDW per unit cell. Therefore, the CFP is the most promising ground state for 5/4 filled Kagome lattice.

Besides the ground state energy comparison, the most unconventional behavior for CDW state in AV_3Sb_5 is the chiral anisotropy found by STM measurements under magnetic field [12]. In addition, the anomalous Hall measurements also point out the CDW should break the time-reversal symmetry [24, 25]. These results support the CFP as the ground state compared to the other two time-reversal conserved charge orders. To confirm this, we calculate the intrinsic Hall responses using the Kubo formula [38–40], which is directly related to the Chern number for each band

$$\sigma_{xy} = \frac{e^2}{\hbar} \sum_{k,n \neq m} \frac{[f(\epsilon_{nk}) - f(\epsilon_{mk})] \text{Im}(v_x^{nm} v_y^{mn})}{(\epsilon_{nk} - \epsilon_{mk})^2} \quad (10)$$

where the $f(x)$ is the Fermi distribution function and $v_{x/y}^{nm} = \langle nk | \hat{v}_{x/y} | mk \rangle$ is the matrix element of the velocity operator. The Chern number for each occupied CFP band is listed in Fig. 2f. The CFP is also a QAH insulator with $C = 1$ for each spin sector. The total Hall response is $\sigma_{xy} = 2 \frac{e^2}{\hbar}$ for the CFP charge order. However, it is important to note that the AV_3Sb_5 is a multi-orbital system, there are Fermi surfaces that are not captured in our simple one-orbital model and can not be fully gapped out by the CFP order. Therefore, the Hall conductance should not be quantized.

The charge density distribution for the CFP state at each site is plotted in Fig. 3a. We find that there are two types of charge sites and two special flux loops. As shown in Fig. 3a, the two anti-clockwise triangle current flux loops (red circles) form a honeycomb lattice and the clockwise hexagonal current flux (blue circle) forms a triangular lattice. The charge density

for each site at the anti-clockwise flux triangular is relatively larger than the charge density at the hexagonal current flux, as indicated in Fig. 3a. This charge distribution clearly gives rise to a 2×2 charge order. Choosing two representative charge sites, we also calculate the tunneling density of states at sites 1A and 2A. They also show distinct features, as plotted in Fig. 3b.

From the symmetry breaking point of view, the normal state of Kagome lattice contains the symmetry $D_{6h} \times \mathcal{T}$ in addition to the translation group $T(\mathbf{a}_1, \mathbf{a}_2)$. The D_{6h} is generated by the C_6 rotation along the z axis, C_2' along y axis and inversion symmetry \mathcal{I} . As summarized in Fig. 1c, the vCDW and CBO break the C_6 rotation down to the $C_{3h} \times \mathcal{T}$ and $D_{3h} \times \mathcal{T}$ respectively. Interestingly, although CFP breaks the \mathcal{T} symmetry, there is still one effective point group symmetry D_{6h}^* generated by the C_6 , \mathcal{I} and $C_2'\mathcal{T}$. Hence, the CFP keeps all the point group symmetry of the normal state by doubling the translation vectors. All these symmetry properties can be further examined by symmetry-selective measurements, like the Kerr effect. In addition, the coupling between the superconductivity and the CFP is highly confined by their symmetry characters. It is an intriguing problem to investigate how this \mathcal{T} breaking symmetry phase correlated with the superconductivity in AV_3Sb_5 in the future. And microscopically, an extended Hubbard model with on-site Hubbard interaction U and the nearest-neighbor Coulomb interaction V is needed to stabilize this CFP solution, which will be considered in our following works.

IV. DISCUSSION AND SUMMARY

The CFP resembles the loop-current order and the d-density wave state for the pseudogap phases in cuprates superconductors proposed by C. Varma and S. Chakravarty et al. respectively [41–44]. For loop current order, a current loop is formed inside one Cu and two O triangle while staggered fluxes are

formed in neighboring Cu square plaquettes for the d-density wave state. Such a loop current or d-density wave can lead to an unusual magnetic order as measured by polarized neutron diffractions [42, 45, 46]. Thus, we believe that the polarized neutron diffraction may find a similar signal for the CFP order in AV_3Sb_5 . This signal is related to the orbital magnetism associated with the chiral flux, which is found to be around $0.01 \frac{e}{2\pi} ta^2$ [39, 47], where a is the lattice constant and e is the electron charge.

In summary, we discuss the possible 2×2 charge order states in AV_3Sb_5 , including vCDW, CBO and CFP. We find the CFP state is the lowest energy state, which naturally gives rise to the time-reversal symmetry breaking and anomalous Hall effect. Our findings will provide a new understanding for the topological CDW state of the Kagome material AV_3Sb_5 .

Conflict of interest

The authors declare that they have no conflict of interest.

Acknowledgments

We thank Jiaxin Yin, Zhenyu Wang, Jinguang Cheng, and Geng Li for useful discussions. This work was supported by the National Basic Research Program of China (2017YFA0303100), the Ministry of Science and Technology of China (2016YFA0302400), the National Natural Science Foundation of China (NSFC-11888101, NSFC-11674370 and NSFC-11674278), Beijing Municipal Science and Technology Commission Project (Z181100004218001), the Strategic Priority Research Program of Chinese Academy of Sciences (XDB28000000 and XDB33000000), and the Information Program of the Chinese Academy of Sciences (XXH13506-202). K.J. acknowledges support from the start-up grant of IOP-CAS. Z.W. is supported by the U.S. Department of Energy, Basic Energy Sciences Grant No. DE-FG02-99ER45747.

Author contributions

Xilin Feng, Kun Jiang, Ziqiang Wang and Jiangping Hu jointly identified the problem, performed the calculations and analysis, and wrote the paper.

-
- [1] Zhou Y, Kanoda K, Ng TK. Quantum spin liquid states. *Rev Mod Phys* 2017;89:025003.
 - [2] Ran Y, Hermele M, Lee PA, et al. Projected-wave-function study of the spin- $\frac{1}{2}$ heisenberg model on the Kagome lattice. *Phys Rev Lett* 2007;98:117205.
 - [3] Helton JS, Matan K, Shores MP et al., Spin dynamics of the spin- $\frac{1}{2}$ Kagome lattice antiferromagnet $ZnCu_3(OH)_6Cl_2$. *Phys Rev Lett* 2007;98:107204.
 - [4] Lin ZY, Choi JH, Zhang Q, et al. Flatbands and emergent ferromagnetic ordering in Fe_3Sn_2 Kagome lattices. *Phys Rev Lett* 2008;121:096401.
 - [5] Yin JX, Zhang SS, Chang GQ, et al. Negative flat band magnetism in a spinorbit-coupled correlated kagome magnet. *Nat Phys* 2019;15:443.
 - [6] Kang MG, Ye LD, Fang SA, et al. Dirac fermions and flat bands in the ideal kagome metal $FeSn$. *Nat Mater* 2020;19:163.
 - [7] Tang E, Mei JW, Wen XG. High-temperature fractional quantum Hall states. *Phys Rev Lett* 2011;106:236802.
 - [8] Ye L, Kang MG, Liu JW, et al. Massive Dirac fermions in a ferromagnetic kagome metal. *Nature* 2018;555:638.
 - [9] Yin JX, Zhang SS, Li H, et al. Giant and anisotropic many-body spinorbit tunability in a strongly correlated kagome magnet. *Nature* 2018;562:91.
 - [10] Ohgushi K, Murakami S, Nagaosa N. Spin anisotropy and quantum Hall effect in the kagome lattice: chiral spin state based on a ferromagnet. *Phys Rev B* 2000;62:R6065(R).
 - [11] Guo HM, Franz M. Topological insulator on the kagome lattice. *Phys Rev B* 2009;80:113102.
 - [12] Yin JX, Ma WL, Cochran TA et al. Quantum-limit Chern topological magnetism in $TbMn_6Sn_6$. *Nature* 2020;583:533.
 - [13] Ortiz BR, Gomes LC, Morey JR, et al. New kagome prototype materials: discovery of KV_3Sb_5 , RbV_3Sb_5 , and CsV_3Sb_5 . *Phys Rev Mater* 2019;3:094407.
 - [14] Ortiz BR, Teicher SML, Hu Y, et al. CsV_3Sb_5 : a Z_2 topological Kagome metal with a superconducting ground state. *Phys Rev Lett* 2020;125:247002.
 - [15] Ortiz BR, Sarte PM, Kenney EM, et al. Superconductivity in the Z_2 kagome metal KV_3Sb_5 . *Phys Rev Mater* 2021;5:034801.

- [16] Yin QW, Tu ZJ, Gong CS, et al. Superconductivity and normal-state properties of Kagome metal RbV_3Sb_5 single crystals. *Chin Phys Lett* 2021;38:037403.
- [17] Zhao CC, Wang LS, Xia W, et al. Nodal superconductivity and superconducting domes in the topological Kagome metal CsV_3Sb_5 . arXiv:2102.08356, 2021.
- [18] Du F, Luo SS, Ortiz BR, et al. Pressure-tuned interplay between charge order and superconductivity in the kagome metal KV_3Sb_5 . arXiv:2102.10959, 2021.
- [19] Chen KY, Wang NN, Yin QW, et al. Double superconducting dome and triple enhancement of T_c in the kagome superconductor CsV_3Sb_5 under high pressure. arXiv:2102.09328, 2021.
- [20] Liang ZW, Hou XY, Ma WR et al. Three-dimensional charge density wave and robust zero-bias conductance peak inside the superconducting vortex core of a kagome superconductor CsV_3Sb_5 . arXiv:2103.04760, 2021.
- [21] Zhao H, Li H, Ortiz BR et al. Cascade of correlated electron states in a kagome superconductor CsV_3Sb_5 . arXiv:2103.03118, 2021.
- [22] Wang Y, Yang SY, Sivakumar PK, et al. Proximity-induced spin-triplet superconductivity and edge supercurrent in the topological Kagome metal. $\text{K}_{1-x}\text{V}_3\text{Sb}_5$, arXiv:2012.05898, 2020.
- [23] Jiang YX, Yin JX, Denner MM, et al. Discovery of unconventional charge order in kagome superconductor KV_3Sb_5 . arXiv:2012.15709, 2020.
- [24] Yang SY, Wang YJ, Ortiz BR, et al. Giant, unconventional anomalous Hall effect in the metallic frustrated magnet candidate, KV_3Sb_5 . *Sci Adv* 2020;6:eabb6003.
- [25] Yu FH, Wu T, Wang ZY, et al. Concurrence of anomalous Hall effect and charge density wave in a superconducting topological kagome metal. arXiv:2102.10987, 2021.
- [26] Martin I, Batista CD. Itinerant electron-driven chiral magnetic ordering and spontaneous quantum Hall effect in triangular lattice models. *Phys Rev Lett* 2008;101:156402 (2008).
- [27] Tao Li, Spontaneous quantum Hall effect in quarter-doped Hubbard model on honeycomb lattice and its possible realization in doped graphene system, *EPL* **97** 37001.
- [28] Hayami S, Motome Y. Multiple-Q instability by $(d - 2)$ -dimensional connections of Fermi surfaces. *Phys Rev B* 2014;90:060402.
- [29] Jiang K, Zhang Y, Zhou S, et al. Chiral spin density wave order on the frustrated honeycomb and bilayer triangle lattice Hubbard model at Half-filling. *Phys Rev Lett* 2015;114:216402.
- [30] Yu SL, Li JX. Chiral superconducting phase and chiral spin-density-wave phase in a Hubbard model on the kagome lattice. *Phys Rev B* 2012;85:144402.
- [31] Nandkishore R, Levitov L, Chubukov A. Chiral superconductivity from repulsive interactions in doped graphene, *Nat Phys* 2012;8:158.
- [32] Wang WS, Xiang YY, Wang QH, et al. Functional renormalization group and variational Monte Carlo studies of the electronic instabilities in graphene near $\frac{1}{4}$ doping. *Phys Rev B* 2012;85:035414.
- [33] Kiesel ML, Platt C, Hanke W, et al. Competing many-body instabilities and unconventional superconductivity in graphene. *Phys Rev B* 2012;86:020507(R).
- [34] Wang WS, Li ZZ, Xiang YY, et al. Competing electronic orders on kagome lattices at van Hove filling. *Phys Rev B* 2013;87:115135.
- [35] Kiesel ML, Platt C, Thomale R. Unconventional fermi surface instabilities in the Kagome hubbard model. *Phys Rev Lett* 2013;110:126405.
- [36] Jiang SH, Mesaros A, Ran Y. Chiral spin-density wave, spin-charge-charge liquid, and $d + id$ superconductivity in $1/4$ -doped correlated electronic systems on the honeycomb lattice. *Phys Rev X* 2014;4:031040.
- [37] Kenney EM, Ortiz BR, Wang C, et al. Absence of local moments in the kagome metal KV_3Sb_5 as determined by muon spin spectroscopy. arXiv:2012.04737, 2020.
- [38] Thouless DJ, Kohmoto M, Nightingale MP, et al. Quantized Hall conductance in a two-dimensional periodic potential. *Phys Rev Lett* 1982;49:405.
- [39] Xiao D, Chang MC, Niu Q. Berry phase effects on electronic properties. *Rev Mod Phys* 2010;82:1959.
- [40] Fukui T, Hatsugai Y, Suzuki H. Chern numbers in discretized Brillouin zone: efficient method of computing (spin) Hall conductances. *J Phys Soc Jpn* 2005;74:1674.
- [41] Chakravarty S, Laughlin RB, Morr DK, et al. Hidden order in the cuprates. *Phys Rev B* 2001;63:094503.
- [42] Varma CM. Pseudogap in cuprates in the loop-current ordered state. *J Phys Condens Matter* 2014;26:505701.
- [43] Varma CM. Non-Fermi-liquid states and pairing instability of a general model of copper oxide metals. *Phys Rev B* 1997;55:14554.
- [44] Varma CM. Theory of the pseudogap state of the cuprates. *Phys Rev B* 2006;73:155113.
- [45] Fauque B, Sidis Y, Hinkov V, et al. Magnetic order in the pseudogap phase of high- T_c superconductors. *Phys Rev Lett* **96**, 197001 (2006).
- [46] Li Y, Baledent V, Barisic N, et al. Unusual magnetic order in the pseudogap region of the superconductor $\text{HgBa}_2\text{CuO}_4 + \delta$. *Nature* 2008;455:372.
- [47] Thonhauser T. Theory of orbital magnetization in solids. *Int J Mod Phys B* 2011;25:1429.